Proceedings of the Canadian Society for Mechanical Engineering International Congress 2021
CSME Congress 2021
June 27-30, 2021, Charlottetown, PE, Canada

Investigations into the effect of heat exchanger volume and geometry on low-temperature Stirling engine performance

Linda Hasanovich[1] and David S. Nobes[1*]
[1]Mechanical Engineering, University of Alberta, Edmonton, Canada
*dnobes@ualberta.ca

Abstract—The Stirling engine is capable of converting any source of thermal energy into kinetic energy, provided there is a temperature difference between the heat source and sink. This makes it an attractive option for utilizing low-temperature sources such as geothermal or waste heat. However, at these low temperatures, below 100 °C, the optimal engine geometry for a Stirling engine is not well known. It is important to be able to select the optimal geometry of key components, such as the heat exchanger, in order to minimize losses that could further reduce the engine efficiency at low-temperatures. To better understand what the optimal geometry of the heat exchanger components is, a Stirling engine is modelled using third-order commercial modelling software (Sage) and trends of engine properties such as power, temperature, and pressure for different heat exchanger geometries are observed. These trends provide insight into the optimal geometry of these components for low-temperature Stirling engines, as well as providing a methodology for evaluating optimal engine geometry for future engines to be built.

Keywords-Stirling engine, numerical modelling, heat transfer

I. INTRODUCTION

Low temperature heat sources, below 100 °C, are potentially a viable source of energy for generating electricity that could have lower carbon emissions. For example, low temperature heat sources are available in abundance in Alberta, including low temperature geothermal or waste heat from industrial processes [1, 2]. The Stirling engine is a potential solution for converting this low temperature energy into electricity, as Stirling engines have been shown to run on temperature differences as low as 0.5 °C and source temperatures below 100 °C [3], and are capable of running off of any heat source as they are a closed cycle.

For a low-temperature Stirling engine, losses are proportionally higher than they are in high-temperature Stirling engines due to the restricted thermal efficiency at low temperatures. Thus, it is important to minimize the losses in the engine. Excess heat exchanger volume can be a significant loss due to its effect on the pressure change in the cycle. However, as the heating and volume change processes in a Stirling cycle overlap in a real engine, it is not a trivial matter to determine what the optimal heat exchanger size is. The optimal heat exchanger needs to maximize heat delivery to the engine while minimizing excess volume and flow losses. To investigate this relationship and see if there is a particular trend in heat exchanger geometry versus engine power for low temperature Stirling engines, a 3^{rd} order Stirling engine model will be used. The results from this modelling will help inform the design of an experimental engine test setup to confirm the model accuracy and the optimal heat exchanger size for a low-temperature Stirling engine.

II. BACKGROUND

The Stirling engine, using the Stirling cycle, is able to convert heat energy into mechanical energy. The ideal Stirling cycle [4, 5] consists of four processes: isothermal expansion, isochoric heat removal, isothermal compression, and isochoric heat addition. In a real Stirling engine these processes overlap somewhat due to the overlapping piston motions in physical implementation. Thus, the real Stirling engine utilizes a pseudo-Stirling cycle [4, 5]. A real Stirling engine uses several components to achieve this cycle, which are shown in Figure 1 for a Gamma-type Stirling engine [4]. The power piston provides the compression and expansion of the gas while the displacer piston shuttles the working fluid inside the engine through the heat exchangers and regenerator to be heated and cooled. The power piston can be connected to either the expansion space or compression space.

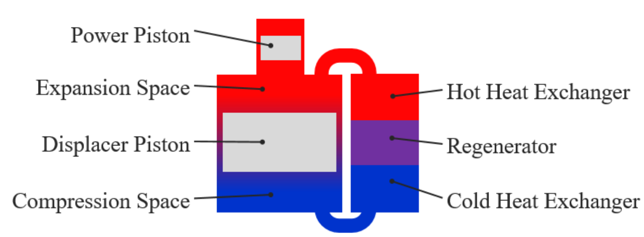

Figure 1. Labelled graphic of Stirling engine components for a Gamma-type engine.

The heat exchangers provide heat input and removal to the working fluid cycling inside the engine. These require the addition of an additional working space volume to the engine,

Future Energy Systems (FES) and the Natural Sciences and Engineering Research Council (NSERC) of Canada.

known as the dead volume. Dead volume is defined as volume that is not swept by either of the pistons [3]. Dead volume is known to contribute to decreased engine power [6] since it is not participating in the heat exchange and volume change processes, and lowers the overall cyclic pressure change in the engine. This is a significant loss present in the Stirling engine that needs to be minimized. However, having too small of a heat exchanger will reduced temperature change in the gas or incur extra flow friction, negatively affecting the performance despite the low dead volume.

III. Modelling Approach

A. *Model Type Selection*

For modelling the real Stirling engine, there are a variety of mathematical models available. They are categorized by Martini [7] according to their complexity and what assumptions they make about the engine processes. A 1st order model is the simplest. It is based on non-dimensional numbers and relates the gas temperatures, engine size and speed to power and efficiency. A 2nd order model is more complex, usually requiring some iteration to solve for power, to which calculated losses are added. Both the 1st and 2nd order models assume the gas temperatures in the engine for the power and loss calculations. A 3rd order model solves the conservation of energy, mass and momentum equations and an equation of state in a one-dimensional form. This is done numerically as these equations are too complex to solve analytically.

For investigating the effect of heat exchanger geometry on engine performance a 3rd order model is used. This is because the 1st and 2nd order models do not capture the tradeoffs of better heat exchange and increased dead volume, as they cannot calculate the gas temperature change associated with additional heat exchanger volume. A 3rd order model captures the potential increase in gas temperature associated with additional heat exchanger volume in a one-dimensional spatial and time varying model.

The 3rd order model that is used in this work is the commercial Stirling engine software Sage created by Gedeon [8]. This has been used for modelling various engines [9] including low-temperature Stirling engines [10], and is able to provide trends of engine power, gas temperatures, and pressure swing for varying heat exchanger geometry.

B. *Model Setup in Sage*

Sage models the Stirling engine as connected components. The connections act as a common boundary value between the two components, for example, equal mass flow. The connections between components is shown in Figure 2. Each component contains relevant relations and variables for that component type.

The conservation equations are solved in Sage on a one-dimensional spatial grid, and the total cells in this grid can be set for each model component. The number of spatial cells for each component is listed in TABLE I. Spaces where there is a steeper temperature gradient or more fine structures, namely the heat exchangers and regenerator, are modelled with more spatial cells in order to better capture the spatial variation. The number of time nodes used for the temporal solution is 15.

TABLE I. Number of nodes in Sage model components

Engine Module	Number of Cells
Expansion Space	3
Displacer Piston and Cylinder	3
Compression Space	3
Power Piston and Cylinder	3
Hot Heat Exchanger	7
Regenerator	11
Cold Heat Exchanger	7

1) *Model Assumptions*

Assumptions of this simplified model are as follows:

- The heat exchanger surfaces are isothermal at the source and sink temperatures specified.
- The flow is one-dimensional.
- The motion of the displacer and power pistons is perfectly sinusoidal.
- The working fluid is dry air represented by the ideal gas law.

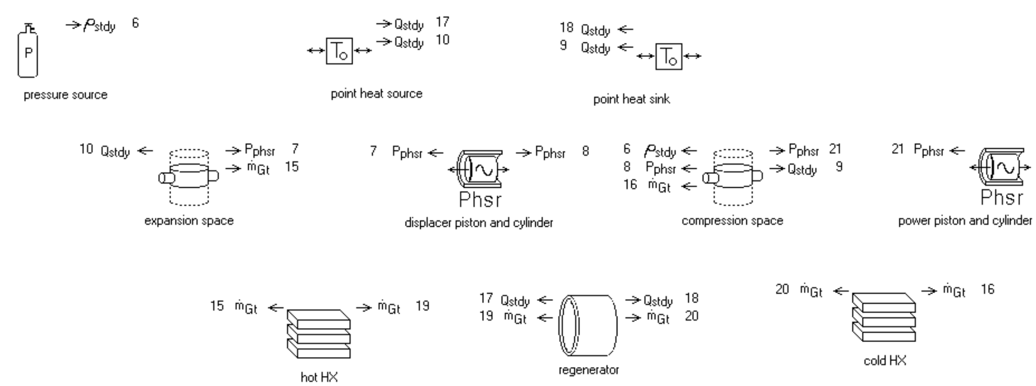

Figure 2. Screen capture of Sage top-level model connections.

In the expansion and compression spaces the thick surface model component is used to model the walls. This represents the quasi-adiabatic condition in the piston, where any heating that occurs with the wall is within a very thin layer.

2) *Engine Operating Conditions*

The engine operating conditions detailed below are summarized in TABLE II.

TABLE II. FIXED ENGINE PROPERTIES

Engine Property	**Value**
Charge Pressure	101.325 kPa
Engine Frequency	1 Hz
Hot Side Temperature	368.2 K
Cold Side Temperature	278.2 K
Displacer Diameter	0.35 m
Displacer Stroke	0.20 m
Power Diameter	0.30 m
Power Stroke	0.30 m
Regenerator Porosity	0.95
Regenerator Wire Diameter	0.00005 m
Regenerator Type	Random Fiber Matrix
Regenerator Diameter	0.18 m
Regenerator Length	0.10 m
Heat Exchanger Channel Width	0.15 m
Heat Exchanger Channel Height	0.001 m

a) *Charge Pressure*

The charge pressure of the engine is chosen to be atmospheric pressure as the planned experimental engine is being designed to run at atmospheric pressure.

b) *Engine Speed*

The engine speed is held constant in this investigation. The engine speed in a real Stirling engine is dependent on the loading of the engine. In Sage, the engine speed is instead prescribed and the power output may vary with engine speed. The engine speed is estimated to be 1 Hz based on the empirical relation by Kolin [3] for a loaded Stirling engine, as well as experimental data for the maximum power of a low-temperature Gamma-type Stirling engine [11].

c) *Hot and Cold Side Temperatures*

The hot side temperature is chosen to be 95 °C as the low temperature heat sources of geothermal and waste heat can be below 100 °C. The cold side temperature is chosen to be 5 °C as that is approximately the average yearly temperature in Edmonton, Alberta [13].

3) *Engine Geometry*

The engine being modelled in Sage is a Gamma-type Stirling engine. The engine size and geometry is based on a planned experimental engine that will be used to verify the results of the modelling done during its design. The experimental engine is likely to be built out of steel, so the chosen engine material for all components of the engine is stainless steel (SS304). The power piston and displacer piston are phased 90° apart. This phase difference of 90° has been shown to be optimal for Gamma-type Stirling engines [11], and power output is not very sensitive to phase angle [12]. The power piston is connected to the compression space in this engine. The engine geometry detailed below is summarized in TABLE II.

a) *Piston Sizes*

The piston diameters and strokes were selected based on the design of the planned experimental engine. The average displacer piston stroke volume of this engine was targeted to be approximately 40 L. The compression ratio (*CR*) of the engine, defined by Kolin [3], is the ratio of the maximum engine volume over the minimum engine volume. It ranges from approximately 1.1 to 1.9 for this study in order to cover a wide range of values. This range is on the order of empirically estimated compression ratios. The Egas [14] estimate calculated from (1) is 1.3 and the Kolin [3] estimate calculated from (2) is 1.1. In these equations T_{hot} is the hot source temperature and T_{cold} is the cold sink temperature, both in units of Kelvin.

$$CR = T_{\mathrm{hot}}/T_{\mathrm{cold}} \tag{1}$$

$$CR = 1 + (T_{\mathrm{hot}}\ \ T_{\mathrm{cold}})/1100 \tag{2}$$

b) *Regenerator Sizing*

The regenerator component acts as temporary storage of thermal energy as the air is shuttled between the hot and cold spaces of the engine. It was sized using the assumption that the energy contained in the mass of air in the engine would need to be stored in the regenerator without allowing a large change in temperature of the regenerator material. A small temperature change in the regenerator material makes the thermal storage process near reversible, which is optimal. Storing the total amount of energy contained in the mass of air in the engine is used as the maximum boundary on regenerator size. This corresponds to a scenario where there are no heat exchangers and the regenerator must store all of the energy in the cycle.

The total amount of energy in the mass of air in the engine is found using:

$$Q = m_{\mathrm{air}} c_{\mathrm{p,air}} (T_{\mathrm{hot}}\ \ T_{\mathrm{cold}}) \tag{3}$$

where Q is the total energy in the air in Joules, m_{air} is the total mass of air in kilograms, and $c_{\mathrm{p,air}}$ is the specific heat capacity taken at the average air temperature in Joules per kilogram per Kelvin.

The mass of regenerator material is then found by equating the total energy of the air in the engine and rearranging the specific heat equation to solve for mass, as:

$$m_{reg} = Q/(c_{p,reg}(T_{hot,reg}\ \ T_{cold,reg})) \tag{4}$$

where $c_{p,reg}$ is the specific heat of the regenerator material. $T_{hot,reg}$ and $T_{cold,reg}$ are the allowable hot and cold regenerator temperatures. In this case, the change in temperature in the regenerator material is limited to within 5 °C of the average air temperature, making the values 55 °C and 45 °C respectively.

The volume of the regenerator was then found using the density of the material to find the solid volume, and then calculating the total volume based on the porosity. The regenerator porosity, calculated as void volume over total volume, was chosen to be 0.95 based on experimental engines with similar regenerators [15], and to lower the overall pressure drop through the regenerator. The regenerator length was chosen to be 0.1 m to match the shortest heat exchanger length examined, and also to minimize the frictional pressure drop through the regenerator. The regenerator diameter was then found from the regenerator length and volume.

The regenerator wire size is representative of the thickness of wire in steel wool [16], which is the type of material that would be used to make this regenerator.

c) Heat Exchanger Geometry

The heat exchanger geometry chosen is an approximate representation of a plate-frame heat exchanger or a bar and plate exchanger that is planned for the experimental engine. This exchanger type has long, narrow slots. These are modelled in Sage as rectangular channel heat exchangers. The length of the slot is the length of the gas path through the heat exchanger and the number of slots in the heat exchanger corresponds to the frontal area. These two parameters represent different sized plates and a different number of plates in a plate-frame heat exchanger.

4) Defined Output Variables

The outputs from Sage that are of interest are:

- Power
- Average Gas Temperature Difference
- 1st Order Expansion Space Pressure Swing
- 1st Order Compression Space Pressure Swing

The output power is defined as the sum of the power output calculated by Sage in the expansion and compression spaces. The average gas temperature difference is defined as the difference between the time and spatially averaged gas temperature in the expansion and compressions spaces. Finally, the pressure swings are approximately determined from the Fourier series solution for pressure. Only the first order amplitude is taken from the Fourier series and used to approximate the pressure swing. The remaining terms of the Fourier series have a diminishing effect on the overall pressure swing and are not considered for this study. Both the compression space and expansion space pressure swings are considered as they are separated by the heat exchangers and regenerator. So, any difference in pressure swing between them would be due to the pressure drop across those components.

IV. METHODOLOGY

For this investigation the heat exchanger length and frontal area are varied, but the geometry of the heat exchanger channels is held constant. The length and frontal area are varied to give different heat exchanger sizes, and it will be possible to see if there is an optimal ratio between these dimensions in addition to total volume. The frontal area is varied by changing the number of slots in the heat exchanger. A summary of the range of heat exchanger lengths and number of slots tested is shown in TABLE III. The model is solved for every possible combination of these parameters.

TABLE III. VARIED ENGINE PROPERTIES

Engine Property	Minimum Value	Maximum Value	Increment
Heat Exchanger Channel Length	0.1 m	0.5 m	0.05 m
Heat Exchanger Number of Slots	100	1000	100

The range of heat exchanger sizes chosen to be explored is based on analysis using the 1st order Schmidt model for Stirling engines as described by Urieli and Berchowitz [4]. The volume of the engine, assumed gas temperatures, and a range of heat exchanger volumes are inputted into the model to determine the power output. The lowest assumed gas temperature difference considered is based on experimental engine data that showed the average hot side and cold side temperatures of the engine [11]. The power output is plotted against dead volume ratio, which is a non-dimensionalized measure of dead volume. Dead volume ratio, defined by Senft [6], is the total engine dead volume divided by the displacer piston swept volume.

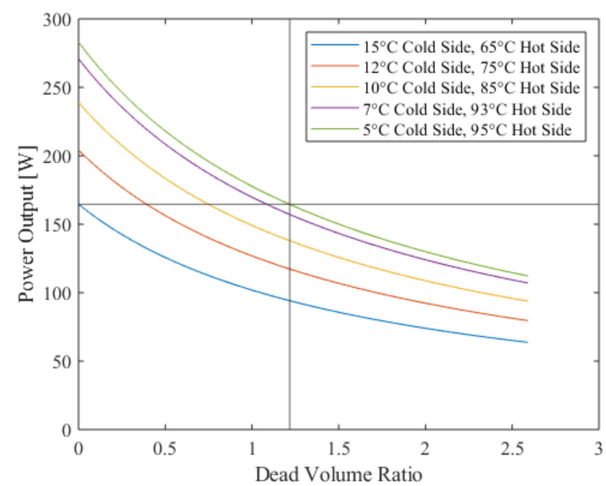

Figure 3. Plot of power output as calculated by the Schmidt model against dead volume ratio for various gas temperature differences.

In Figure 3, it can be seen that by changing the assumed gas temperatures to increase the temperature difference between them, the power output increases for all dead volumes. The maximum power output occurs when the gas temperature reaches the temperature of the source and sink, which is shown by the green line. In order to achieve a greater temperature difference in reality, the heat exchanger volume can be increased. It can be seen that there is a point, marked by the black cross lines, at which any improved heat exchange associated with a larger heat exchanger volume will not be able to provide a larger power output than the smallest heat exchanger with the lowest assumed gas temperature difference considered. This is due to the effect of the increase in dead volume. Thus, the dead volume ratio range tested must have a maximum bound of at least 1.2 for the lowest gas temperature difference assumed here. The largest heat exchanger geometry investigated corresponds to a dead volume ratio of 7.9, which is much higher and will be able to account for any variation between the assumed lowest gas temperature difference and the one calculated by the model.

The lowest heat exchanger volume is limited by the physical length requirements of the heat exchanger for the planned experimental engine, as well as the ability of the model to solve for a very small heat exchanger. Due to this, the lowest dead volume ratio considered was 0.3.

V. RESULTS

Preliminary results from the model show that there is an optimum size for the heat exchanger volume to produce maximum power. In Figure 4, it can be seen that the maximum engine power of 22.2 W occurs for a heat exchanger length of 0.1 m with 400 or 500 slots. This is a dead volume ratio range of 0.75 to 0.91. This dead volume ratio range is also within the maximum bound predicted by the Schmidt model. It should be noted that negative power produced by the model indicates that the engine as modelled would not run, and would take that amount of energy to be forced to run at the given conditions.

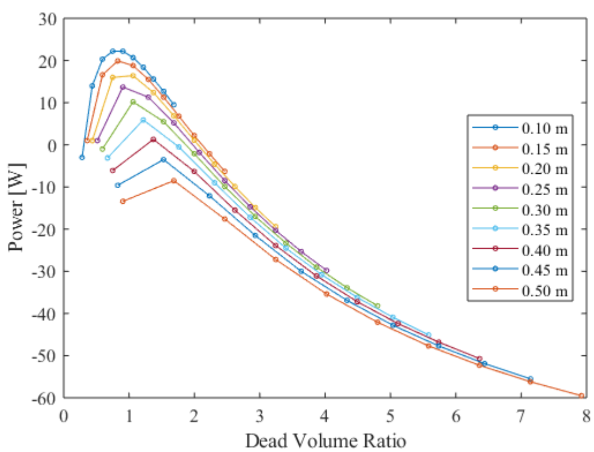

Figure 4. Engine power from Sage against dead volume ratio for various heat exchanger lengths.

In Figure 5, it can be seen that the gas temperature difference between the hot side and the cold side does increase and then plateau for the heat exchanger size. This is expected as the maximum temperature difference that could be achieved by the heat exchangers is 90 °C, so the temperature difference will asymptote to that value as there is more heat exchange power available. The temperature difference will continue to increase with increased heat exchanger size.

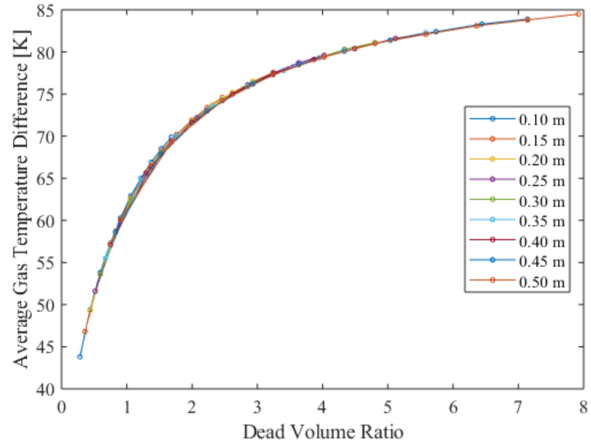

Figure 5. Average gas temperature difference against dead volume ratio for various heat exchanger lengths.

In Figures 6 and 7 the compression and expansion space pressure swings respectively are plotted against the dead volume ratio. The pressure swing is the difference between the maximum and minimum pressure during the cycle. In both figures it can be seen that the pressure swing in the engine decreases significantly with increased heat exchanger volume.

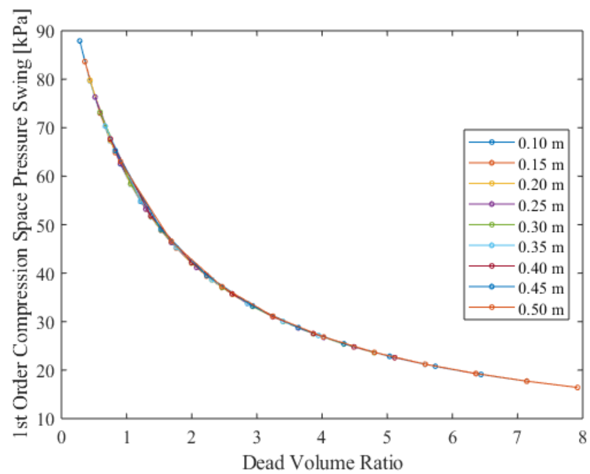

Figure 6. 1st order compression space pressure swing against dead volume ratio for various heat exchanger lengths.

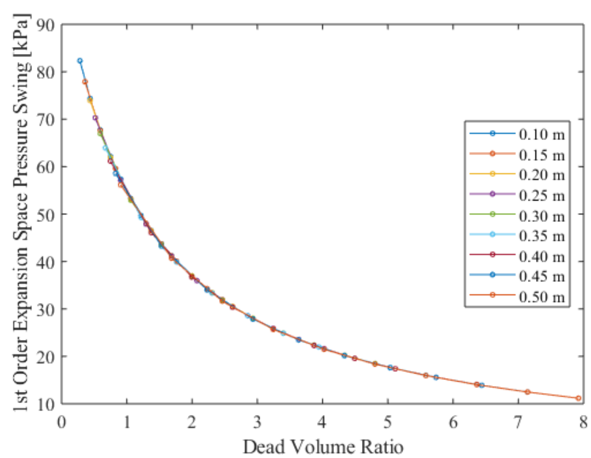

Figure 7. 1st order expansion space pressure swing against dead volume ratio for various heat exchanger lengths.

This contributes to the overall decrease in engine power despite the increased gas temperature difference. In Figure 7, it can also be seen that the expansion space pressure swing is lower than the compression space pressure swing seen in Figure 6. This is due to the pressure loss through the heat exchanger and regenerator components.

These results also indicate that shorter heat exchangers produce higher engine power than long heat exchangers, as long as both are capable of generating a similar gas temperature difference. TABLE IV. compares the pressure swing, gas temperature difference, and power for the same dead volume ratio of 0.91 for maximum power. This table shows that there is a decrease in the pressure swing in the expansion space of the engine while the compression space pressure swing increases. This would result in a higher power output for the shorter heat exchanger length as the expansion space would do more work for a smaller amount of compression space work. This result indicates that pressure drop through the heat exchangers has a significant effect on power output, provided that the heat exchanger geometry chosen is able to transfer the energy to and from the working fluid effectively.

TABLE IV. COMPARISON OF IDENTICAL DEAD VOLUME RATIOS WITH DIFFERENT HEAT EXCHANGER SIZES.

Properties	Heat Exchanger Size	
	Short Heat Exchanger	***Long Heat Exchanger***
Heat Exchanger Length	0.1 m	0.5 m
Number of Slots in Heat Exchanger	500	100
Temperature Difference	60.3 K	60.1 K
Compression Space Pressure Swing	62.5 kPa	63.0 kPa
Expansion Space Pressure Swing	57.4 kPa	56.2 kPa
Power	22.2 W	-13.4 W

VI. CONCLUSION

From the results of this investigation of a low-temperature Stirling engine using a 3^{rd} order model we can gain insight into the trends in engine power for varying heat exchanger volumes. The optimal dead volume ratio for this engine was between 0.75 and 0.91, with a short heat exchanger length of 0.1m and 400 to 500 slots. The shorter path length heat exchangers resulted in high power output due to the decreased pressure drop through the heat exchanger for equivalent gas temperature difference to a heat exchanger with longer path length. This information can help provide a recommended heat exchanger size to be used for an experimental engine to provide optimal power output, particularly in the case of low-temperature Stirling engines in which maximizing power output is of great importance.

Future work includes studying different heat exchanger and engine geometries as well as different engine operating conditions to gain further understanding on the influence of these factors on the optimal heat exchanger geometry for a low-temperature Stirling engine.

ACKNOWLEDGMENT

The authors acknowledge financial support from Future Energy Systems (FES) and the Natural Sciences and Engineering Research Council (NSERC) of Canada.

REFERENCES

[1] J. Banks, “Deep-Dive Analysis of the Best Geothermal Reservoirs for Commercial Development in Alberta : Final Report,” University of Alberta, Edmonton, 2017.

[2] “Community Integrated Energy Mapping Feasability Study in Alberta's Industrial Heartland and Strathcona Industrial Area,” June 2014. Available: http://cmcghg.com/wp-content/uploads/2015/03/EEBE-062-Report-Short-EN.pdf

[3] I. Kolin, Stirling Motor: History - Theory - Practice, Zagreb University Publications, Ltd., Dubrovnik, 1991.

[4] I. Urieli and D. Berchowitz, Stirling Cycle Engine Analysis, Adam Hilger Ltd, Bristol, 1984.

[5] L. Červenka, “Idealization of the Real Stirling Cycle,” J. of Middle European Construction and Design of Cars, vol. 14, no. 3, pp. 19-27, 2016.

[6] J. Senft, Mechanical Efficiency of Heat Engines, Cambridge University Press, Cambridge, 2007

[7] W. Martini, “Stirling Engine Design Manual”, 2nd ed., January 1983.

[8] D. Gedeon, “Sage: Object Oriented Software for Stirling Machine Design,” Proceedings of the Intersociety Energy Conversion Engineering Conf., USA, pp. 1902-1907, August 1994

[9] R. Demko and L. Penswick, “Sage Simulation Model for Technology Demonstration Convertor by a Step-by-Step Approach,” 3rd Int. Energy Conversion Engineering Conference, August 2005.

[10] B. Hoegel, D. Pons, M. Gschwendtner, A. Tucker and M. Sellier, “Thermodynamic peculiarities of alpha-type Stirling engines for low-temperature difference power generation: Optimisation of operating parameters and heat exchangers using a third-order model”, Proceedings of the Institution of Mechanical Engineering, Part C: Journal of Mechanical Engineering Science, vol. 228, no. 11, pp. 1935-1947, 2014.

[11] C. Stumpf, “Parameter Optimization of a Low Temperature Difference Gamma-Type Stirling Engine to Maximize Shaft Power”, Thesis.

[12] J. Senft, “Optimum Stirling engine geometry,” Int. J. of Energy Research, vol. 26, no. 12, pp. 1087-1101, 2002.

[13] “Canadian Climate Normals 1981-2010 Station Data,” Government of Canada, December 10, 2020. [Online]. Available: https://climate.weather.gc.ca/climate_normals/results_1981_2010_e.html?searchType=stnProv&lstProvince=AB&txtCentralLatMin=0&txtCentralLatSec=0&txtCentralLongMin=0&txtCentralLongSec=0&stnID=1865&dispBack=0

[14] J. Egas, “Stirling Engine Configuration Selection,” Energies, vol. 11, no. 584, pp. 1–23, 2018.

[15] R. Gheith, F. Aloui and S. Nasrallah, “Determination of adequate regenerator for a Gamma-type Stirling engine,” Applied Energy, vol. 139, pp. 272-280, February 1, 2015.

[16] “Steel Wool Grades,” Engineering Toolbox, 2010. [Online]. Available: https://www.engineeringtoolbox.com/steel-wool-grades-d_1619.html